

2018

## Bilayer thickness and curvature influence binding and insertion of a pHLIP<sup>®</sup> peptide

Alexander G. Karabadzhak

Dhammika Weerkkody  
*University of Rhode Island*

John Deacon

Oleg A. Andreev  
*University of Rhode Island, andreev@uri.edu*

Yana K. Reshetnyak  
*University of Rhode Island, reshetnyak@uri.edu*

*See next page for additional authors*

Follow this and additional works at: [https://digitalcommons.uri.edu/phys\\_facpubs](https://digitalcommons.uri.edu/phys_facpubs)

---

### Citation/Publisher Attribution

Karabadzhak, A. G., Weerkkody, D., Deacon, J., Andreev, O. A., Reshetnyak, Y. K., & Engelman, D. M. (2018). Bilayer thickness and curvature influence binding and insertion of a pHLIP<sup>®</sup> peptide. *Biophysical Journal*, 114(9), 2107-2115. doi: 10.1016/j.bpj.2018.03.036  
Available at: <https://doi.org/10.1016/j.bpj.2018.03.036>

This Article is brought to you by the University of Rhode Island. It has been accepted for inclusion in Physics Faculty Publications by an authorized administrator of DigitalCommons@URI. For more information, please contact [digitalcommons-group@uri.edu](mailto:digitalcommons-group@uri.edu). For permission to reuse copyrighted content, contact the author directly.

---

## Bilayer thickness and curvature influence binding and insertion of a pHLIP<sup>®</sup> peptide

### Authors

Alexander G. Karabadzhak, Dhammika Weerkkody, John Deacon, Oleg A. Andreev, Yana K. Reshetnyak, and Donald Engelman

The University of Rhode Island Faculty have made this article openly available.  
Please let us know how Open Access to this research benefits you.

This is a pre-publication author manuscript of the final, published article.

### Terms of Use

This article is made available under the terms and conditions applicable towards Open Access Policy Articles, as set forth in our [Terms of Use](#).

# **Bilayer thickness and curvature influence binding and insertion of a pHLIP<sup>®</sup> peptide**

Alexander G. Karabadzhak<sup>1</sup>, Dhammika Weerakkody<sup>2</sup>, John Deacon<sup>1</sup>,  
Oleg A. Andreev<sup>2</sup>, Yana K. Reshetnyak<sup>2</sup>, Donald M. Engelman<sup>1</sup>

<sup>1</sup>Department of Molecular Biophysics and Biochemistry, Yale University, P.O. Box 208114,  
New Haven, CT 06520, USA

<sup>2</sup>Physics Department, University of Rhode Island, 2 Lippitt Rd., Kingston, RI 02881, USA

## **Corresponding authors:**

Donald M. Engelman, Department of Molecular Biophysics and Biochemistry, Yale University,  
266 Whitney Ave., New Haven, CT, 06511, USA, Phone: (203) 432-5601, Fax: (203) 432-6381,  
e-mail: [donald.engelman@yale.edu](mailto:donald.engelman@yale.edu)

Yana K. Reshetnyak, Physics Department, University of Rhode Island, 2 Lippitt Rd., Kingston,  
RI, 02881, USA, Phone (401) 874-2060, Fax: (401) 874-2380, e-mail: [reshetnyak@uri.edu](mailto:reshetnyak@uri.edu)

## **Abstract**

The physical properties of lipid bilayers, such as curvature and fluidity, can affect the interactions of polypeptides with membranes, influencing biological events. Additionally, given the growing interest in peptide-based therapeutics, understanding the influence of membrane properties on membrane associated peptides has potential utility. pH Low Insertion Peptides (pHLIPs) are a family of water soluble peptides that can insert across cell membranes in a pH-dependent manner, enabling the use of pH to follow peptide-lipid interactions. Here we study pHLIP interactions with liposomes varying in size and composition, in order to determine the influence of several key membrane physical properties. We find that pHLIP binding to bilayer surfaces at neutral pH is governed by the ease of access to the membrane's hydrophobic core, which can be facilitated by membrane curvature, thickness and the cholesterol content of the membrane. Following surface binding, if the pH is lowered, the kinetics of pHLIP folding to form a helix and subsequent insertion across the membrane depends on the fluidity and energetic dynamics of the membrane. We showed that pHLIP is capable of forming a helix across lipid bilayers of different thickness at low pH. However, the kinetics of the slow phase of insertion corresponding to the translocation of C-terminal end of the peptide across lipid bilayer, vary ~ 2-fold, and correlate with bilayer thickness and fluidity. While these influences are not large, local curvature variations in membranes of different fluidity could selectively influence surface binding in mixed cell populations.

## Introduction

Helical transmembrane proteins constitute ~ 30% of all proteins coded in the genome [1]. The study of polypeptide insertion into biological membranes can advance our understanding of membrane protein stability and folding, and also has potential practical applications. However, experimental studies have historically been challenging because peptides that are lipophilic enough to form transmembrane helices are typically insoluble in aqueous solution. Biological membranes are also diverse and complex, with anisotropic transmembrane compositions, making evaluation of interactions using model systems difficult [2]. Importantly, a bilayer's physical properties can significantly influence the form and function of membrane associated proteins [3, 4]. As a consequence of these complications, the mechanistic and energetic properties of the interactions between transmembrane peptides and biological membranes are not well understood. Some of the variation in biological membrane phospholipids is in their acyl chain length and degree of saturation. Acyl chain length and saturation contribute to bilayer thickness and membrane fluidity [5]. Cholesterol is another significant component in eukaryotic plasma membranes that modulates lipid dynamics [6, 7]. The influence of lipid bilayer properties on the interactions of membrane peptides have only been thoroughly studied for a few cases. The most investigated transmembrane proteins are bacteriorhodopsin and OmpA [8]. Previous studies, largely using phosphatidyl choline (PC) with different hydrocarbon chains, have established that lipid properties can influence the kinetics of insertion and formation of secondary structures in these two proteins. For example, bacteriorhodopsin folding efficiency can be altered by changing the phospholipid head groups as well as by changing their acyl chain length [9, 10]. The folding was suppressed in *diC*<sub>14:0</sub>PC lipids compared to longer *diC*<sub>18:1</sub>PC and *diC*<sub>16:0</sub>PC lipids. In another study, the folding yield and rates of the membrane protein, diacylglycerol kinase, was reduced by shortening the acyl chain length of PC lipids [11]. Several studies on spontaneous folding of the  $\beta$ -barrel OmpA protein showed its dependence on the thickness of the membrane bilayer [12, 13]. In particular, the kinetics of secondary structure formation of the protein, FomA, strongly depends on bilayer thickness and was slower in *diC*<sub>12</sub>PC compare to lipids with longer acyl chains [12].

pH Low Insertion Peptides (pHLIPs) provide an opportunity to examine surface binding and pH-triggered folding across membranes. pHLIPs enable the study of membrane influences on

peptide interactions by being stable as soluble monomers in water at neutral or basic pH while responding to low pH by inserting across membranes as a transmembrane  $\alpha$ -helix. pHLIPs exist in three major equilibrium states: (State I) soluble in water as a mostly unstructured monomer, (State II) bound to the surface of a lipid bilayer as a mostly unstructured monomer, and (State III) inserted across the bilayer as an  $\alpha$ -helix [14]. The exact configuration of the peptide in each state depends on the pHLIP sequence. The greatest variability is observed for various pHLIP peptides adsorbed at the membrane bilayer in State II. The existence of these three distinct equilibrium states makes it possible to separate the process of the peptide's attachment to a lipid bilayer from the process of the peptide's insertion/folding.

The transition from the membrane bound State II to the transmembrane State III is controlled by the protonation of carboxyl groups in a pHLIP's transmembrane domain and, transiently, in the membrane-inserting end of the peptide [15-17]. The negative charges on these acidic sidechains in neutral or basic environments prevent the stable presence of the transmembrane domain across the nonpolar membrane core. However, in acidic environments these sidechains are fully or partially protonated, promoting insertion and stabilization of the transmembrane helix [18]. Thus, the insertion/folding and exit/unfolding of the pHLIP peptides can be triggered by changing the pH, enabling kinetic studies. Insertion kinetics of wild-type (WT) pHLIP is well described by a four-state model, which assumes a sequential pathway for the processes of insertion that starts from State II and proceeds to final State III via two intermediates (Int<sub>1</sub> and Int<sub>2</sub>) [17].

Because pHLIPs sense acidity and tumors are acidic, applications are being pursued for tumor-targeted therapies, diagnostics and research tools [19-23]. Understanding the influence of membrane properties on pHLIPs thus illuminates both basic principles of membrane biology and practical knowledge that may prove useful for the development of pHLIP-based technologies.

Here we present a study of pHLIP interaction with bilayers composed of different monounsaturated PC lipids (*diC*<sub>14:1</sub>PC, *diC*<sub>16:1</sub>PC, *diC*<sub>18:1</sub>PC, *diC*<sub>20:1</sub>PC *diC*<sub>22:1</sub>PC), in the presence and absence of cholesterol, to explore the influences of lipid bilayer properties on pHLIP binding to membrane surfaces and transmembrane helix insertion.

## **Materials and Methods**

### **Synthesis of pHLIP peptides**

The pHLIP peptide (H<sub>2</sub>N–GGEQNPIYWARYADWLFTTPLLALLDLALLVDADEGT–COOH) was prepared by solid-phase peptide synthesis using Fmoc (9-fluorenylmethyloxycarbonyl) chemistry and purified by reverse phase chromatography at the W.M. Keck Foundation Biotechnology Resource Laboratory at Yale University. Lyophilized peptide was dissolved in a solution containing 3 M urea to denature any aggregates, then exchanged into 10 mM phosphate buffer, pH 8.0 using a G-10 size-exclusion fast spin column. The peptide concentration was determined by absorbance ( $\epsilon_{280} = 13,940 \text{ M}^{-1} \text{ cm}^{-1}$ ).

### **Liposome preparation**

Lipids were purchased from Avanti Polar Lipids (biological source/molecular names and catalogue numbers in parentheses): 14:1-PC (1,2-dimyristoleoyl-sn-glycero-3-phosphocholine, 850,346C), 16:1-PC (1,2-dipalmitoleoyl-sn-glycero-3-phosphocholine, 850,358C), 18:1-PC (1,2-dioleoyl-sn-glycero-3-phosphocholine, 850,375C), 20:1-PC (1,2-dieicosenoyl-sn-glycero-3-phosphocholine, 850,396C) and 22:1-PC (1,2-dierucoyl-sn-glycero-3-phosphocholine, 850,398C). Small, large and giant unilamellar vesicles (SUVs, LUVs and GUVs) were prepared by extrusion. Lipids, with or without cholesterol, were dissolved in chloroform and desolvated on a rotary evaporator, and then dried under high vacuum for several hours. The phospholipid film was rehydrated in 10 mM phosphate buffer, pH 8.0, vortexed into suspension, and the suspension was repeatedly extruded using 50 nm, 100 nm, 200 nm or 1  $\mu\text{m}$  membrane pore filters (Avanti Polar Lipids).

### **Steady-state fluorescence and circular dichroism measurements**

Fluorescence and circular dichroism (CD) measurements were employed to observe the partitioning of the peptide into a lipid bilayer and the formation of helical structure, respectively, according to previously established experimental protocols [14]. Tryptophan fluorescence and circular dichroism (CD) measurements were carried out on a PC1 photon counting spectrofluorimeter (ISS, Inc.) and a MOS-450 spectropolarimeter (Biologic, Inc.), respectively, under temperature control. All measurements were performed at 25°C. Peptide fluorescence spectra were recorded from 310 nm to 410 nm with the spectral widths of excitation and emission slits set at 4 nm and 2 nm, respectively, using a 295 nm excitation wavelength. The

polarizers in the excitation and emission paths were set at the “magic” angle (54.7° from the vertical orientation) and vertically (0°), respectively, to reduce Wood’s anomalies from the reflecting holographic grating. Peptide CD spectra were recorded from 190 nm to 270 nm with 1 nm increments using a sample cuvette with an optical path length of 0.5 cm.

A stock solution of pHLIP (typically 20 – 30 μM) in 10 mM pH 8.0 phosphate buffer was mixed with a stock solution of liposomes (typically 3 mM) in 10 mM pH 8.0 phosphate buffer to obtain a final solution with concentrations of the peptides and lipids of 2 μM and 0.4 mM, respectively. The peptide-lipid solution was equilibrated at 4°C overnight before any measurements were made. For membrane curvature comparison measurements the concentration of peptides and lipids were 4 μM and 0.8 mM, respectively and the fluorescence excitation wavelength was set at 280 nm to reduce amount of scattered signal. The selected peptide:lipid ratio of 1:200 ensures that most of the pHLIP peptides are adsorbed at the surface of lipid bilayers as was established in our previous studies [15].

#### **Fluorescence anisotropy measurements**

LUVs were prepared from 14:1PC, 16:1PC, 18:1PC, 20:1PC, 22:1PC lipids, with or without cholesterol, according to the protocol described above. pHLIP (2 μM) was added to solutions to give a final pHLIP/lipid molar ratio of 1:200 and the mixture was left overnight to equilibrate. Tryptophan fluorescence polarization was measured on a PC1 photon counting spectrofluorimeter (ISS, Inc.) at 25°C. The widths of excitation and emission slits were 4 nm. Excitation and emission wavelengths were set to 280 nm and 350 nm, respectively. Fluorescence emission was recorded for 1 min and averaged 10 times. The vertically and horizontally polarized emission intensities were corrected for background scattering by subtraction of the corresponding polarized intensities of a blank containing a LUVs suspension without pHLIP. Steady-state fluorescence anisotropy was determined according to the following equation:

$$r = \frac{I_{VV} - GI_{VH}}{I_{VV} + 2GI_{VH}}$$

where  $I_{VV}$  and  $I_{VH}$  are the emission intensities measured with the excitation polarizer set in the vertical direction and the emission polarizer oriented in the vertical or horizontal directions,



respectively. The instrumental factor  $G$  ( $G = I_{HV} / I_{HH}$ ) was determined by measuring the emission intensities of a solution of the fluorescent probe with the excitation polarizer oriented in the horizontal direction.

### **Oriented circular dichroism measurements**

Oriented circular dichroism was measured from supported bilayers deposited on quartz slides with a special polish for far-UV measurements and with 0.2 mm spacers on one side of each slide (Starna) as previously described [18]. Quartz slides were cleaned by i) sonication for 10 min in diluted cuvette cleaner solution Contrad (Decon Labs); ii) rinsing with deionized water ( $\geq 18.2 \text{ M}\Omega \text{ cm}$  at  $25 \text{ }^\circ\text{C}$ ; Milli-Q Type 1 Ultrapure Water System, EMD Millipore); iii) bath sonication for 10 min in 2-propanol; iv) rinsing with deionized water; v) bath sonication for 10 min in acetone; vi) followed by sonication for 10 min in 2-propanol; and vii) rinsing with deionized water; viii) finally, cleaned slides were immersed in Piranha solution (3:1 solution of sulfuric acid to hydrogen peroxide) for 5-10 min to completely remove any remaining organic material from the slides; and, finally, ix) the slides were thoroughly rinsed with and stored in deionized water. A lipid monolayer was deposited on the quartz substrate by the Langmuir-Blodgett (LB) method using a KSV Minithrough. For the LB deposition, a lipid solution in chloroform was spread on the subphase (Milli-Q purified water kept at  $25 \text{ }^\circ\text{C}$ ) and the solvent was allowed to evaporate for about 30 min, followed by monolayer compression to  $32 \text{ mN/m}$ . The first layer was then deposited by retrieving the slide from the subphase at a rate of  $15 \text{ mm/min}$ . The second layer of the bilayer was created by fusion. For this step, the monolayer on the slide was incubated with a solution of lipid vesicles (50 nm in diameter obtained by extrusion) mixed with the peptide solution at the desired pH (0.5 mM PC and  $10 \text{ }\mu\text{M}$  peptide). The fusion was allowed to proceed for about 6 hours at 100% humidity. Then, excess vesicles were removed and the slides were stacked and filled with the peptide solution ( $5 \text{ }\mu\text{M}$ ) at the same pH as pH of the sample used for fusion. Then the bilayers with the peptide solution were allowed to equilibrate for about 6 hours. Measurements were taken at 3 stages: when the monolayers were incubated with excess liposomes, soon after the spaces between slides were filled with the peptide solution and again 6 hours after this second measurement. 12 slides (24 bilayers) were assembled and OCD spectra were recorded using a MOS-450 spectropolarimeter (BioLogic).

Measurements of control samples of lipid bilayers without peptide were used for background correction.

### **Kinetics fluorescence measurements**

Kinetics fluorescence measurements were carried out on a SFM-300 mixing stopped-flow apparatus connected to a MOS-450 spectrometer (Biologic, Inc.) under temperature control as previously described [17, 18]. The FC-20 observation cuvette was used. All solutions were degassed several minutes under vacuum before loading into the syringes to minimize air bubbles. 4  $\mu\text{M}$  solution of pHLIP was pre-incubated with liposomes made from each of the chain length series of Phosphatidyl Cholines (14:1PC, 16:1PC, 18:1PC, 20:1PC, 22:1PC) (0.8 mM of lipids) and 18:1 PC with 20% of cholesterol at pH 8.0 to reach equilibrium in State II, and folding/insertion was induced by fast mixing (5 ms dead time) of equal volumes of the pHLIP-liposome mixture at pH 8.0 and appropriately diluted HCl, to give a pH drop from pH 8.0 to pH 3.6. The final peptide and lipid concentrations were 2  $\mu\text{M}$  and 0.4 mM, respectively. Changes in tryptophan fluorescence were recorded through a 320 nm long-pass filter using an excitation wavelength of 295 nm. The fluorescence signal was corrected for photobleaching. Each kinetic curve was recorded several times and then averaged, excluding the first 2–3 shots. The signals were normalized to a starting point of 1 by using the baseline kinetics recorded at pH 8.0. In most cases these samples were then used for steady-state fluorescence measurements recorded on a PC1 photon counting spectrofluorimeter.

In control experiments we found that liposome size (50 nm or 100 nm) does not detectably affect the state II to state III kinetics of peptide insertion into a membrane. Different peptide:lipid ratios, such as 1:200 and 1:350, were investigated and no difference in kinetics was observed. Different pH jumps from pH8 to pH3 or from pH8 to pH4 also do not affect kinetics runs.

### **Data analysis**

All data were fit to the appropriate equations by nonlinear least squares curve fitting procedures employing the Levenberg Marquardt algorithm using Origin 8.5.

## **Results**

In order to explore lipid effects on the surface binding and transmembrane transition of a peptide as it enters a bilayer, we used pH-triggered insertion of a pHLIP peptide, observing the processes by optical spectroscopy. First, equilibrium studies on peptide-lipid systems were carried out. We varied lipid chain length, cholesterol content, and vesicle curvature using five different lipids *diC*<sub>14:1</sub>PC, *diC*<sub>16:1</sub>PC, *diC*<sub>18:1</sub>PC, *diC*<sub>20:1</sub>PC, and *diC*<sub>22:1</sub>PC (Supplementary Figure S1). Cholesterol content ranged from 0 to 30%, and liposome sizes ranged from 50 to 1000 nm in diameter. The binding of pHLIP to the lipid bilayer at the high pH (State II) was monitored by the shift of the pHLIP fluorescence spectra to shorter wavelengths, which reflects the transfer of tryptophan fluorophores from aqueous solution to a more hydrophobic membrane surface environment [24]. The emission maximum was 351-352 nm for pHLIP interacting with large liposomes (1000 nm in diameter) of different compositions, indicating significant exposure of tryptophan residues to water (Figure 1a). On the other hand, a more blue shifted fluorescence was observed when pHLIP was bound to membranes of greater curvature (i.e. smaller diameter), and much less variability (less than 2 nm shift of the fluorescence maximum ) was seen for the interactions of pHLIP with vesicles of different sizes composed of short acyl chain *diC*<sub>14:1</sub>PC lipids. We also observed progressively larger blue shifts of pHLIP fluorescence in liposomes composed of *diC*<sub>18:1</sub>PC lipids containing increasing amounts of cholesterol (up to 30%) (Figure 1b). Increasing cholesterol content decreases membrane fluidity, especially in the vicinity of membrane surface, and increases lipid bilayer thickness [7].

We have emphasized the study of pHLIP interactions with small liposomes (50 nm in diameter), since small vesicle diameter minimizes the contribution of the light scattering signal in kinetics experiments. In small vesicles, a blue shift of the position of the pHLIP fluorescence maximum at pH 8 correlates with a decrease of bilayer thickness (Supplementary Figure S2a and Figure 2a). CD measurements show formation of peptide helical structure in the presence of liposomes composed of lipids of different acyl chain lengths at low pH (Supplementary Figure S2b). The increase of helicity was monitored by the appearance of CD signal at 222 nm and presented as ratio of CD signal at 222 nm to 208 nm (Figure 2b) [25-27]. The increasing 222/208 nm CD ratio with increasing acyl chain length at pH 8 indicates the appearance of peptide helical content. The helicity of the state II peptide in thick bilayers approaches that of the inserted form in state III. At the same time, the fluorescence anisotropy varies just slightly, within a range from 0.06 to 0.07,

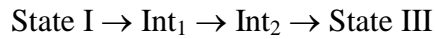
with a maximal value observed for *diC*<sub>18:1</sub>PC liposomes at pH 8 (Figure 2c). The values obtained for the fluorescence anisotropy (close to zero) reflect a rather high flexibility of tryptophan residues in State II. Despite the fact that fluorescence anisotropy measurements were carried out at long wavelength (350 nm), the absolute values obtained for the fluorescence anisotropy should be treated with caution, since polarized emission intensities were corrected for background scattering (see Methods).

Several significant spectral changes are seen with a drop of pH from pH 8 to pH 4: i) the fluorescence intensity increases, ii) a short-wavelength shift of the emission maximum, iii) an increase of fluorescence anisotropy, and iv) helicity increases (Supplementary Figure S2 and Figure 2). These signals are each consistent with the formation and partitioning of helical peptide structures into the lipid bilayer. pHLIP interacting with membranes comprised of long lipids, *diC*<sub>20:1</sub>PC and *diC*<sub>22:1</sub>PC, exhibited reduced quantum yields and the smallest fluorescence anisotropy values in State III compared to the liposomes of thinner bilayers. Quantum yield or fluorescence intensity correlates with the degree of tryptophan residue's exposure to potential quenchers, such as polar and flexible water molecules, reflecting less exposure of pHLIP to aqueous solution in thicker bilayers.

The formation of a helix in State III does not, by itself, establish that the helix has a transmembrane orientation. To determine the orientation of the pHLIP  $\alpha$ -helix with respect to the bilayer plane at low pH, we recorded oriented circular dichroism (OCD) spectra [28]. When pHLIP was incubated with supported bilayers made of *diC*<sub>14:1</sub>PC, *diC*<sub>18:1</sub>PC and *diC*<sub>22:1</sub>PC lipids at pH 3.6, a characteristic OCD spectrum corresponding to the transmembrane orientation was obtained for each lipid type with positive and negative bands around 197 nm and 222 nm, respectively, and the absence of a 208 nm band (Figure 3). Since pHLIP was in its helical configuration when interacting with a thick bilayer, especially *diC*<sub>22:1</sub>PC liposomes in state II (at pH 8), we performed comparative OCD measurements at high and low pHs (Supplementary Figure S3 ). In contrast to the transmembrane helical orientation that the peptide adopts at low pH, a surface helical orientation was observed at high pH in State II, since OCD spectrum recorded at high pH has both negative peaks, at 208 nm and 222 nm, corresponding to a membrane-surface helix [28]. To keep a focus on bilayer variables, we emphasize examination

of pHLIP insertion into membranes composed of *diC*<sub>14:1</sub>PC, *diC*<sub>16:1</sub>PC, and *diC*<sub>18:1</sub>PC lipids, which are associated with the coil to helix transition, and completed by the formation of stable transmembrane helix. By having three comparable transitions we cover a range of bilayer properties that more closely resembles biological membranes.

We found that pHLIP insertion kinetics is highly dependent upon membrane composition and membrane fluidity (Supplementary Figure S4 ). Stopped-flow kinetic studies were based on the following changes in the tryptophan fluorescence of pHLIPs interacting with liposomes of various lipid compositions and liposomes of *diC*<sub>18:1</sub>PC lipids in the presence of 20% cholesterol. The excitation wavelength was set at 295 nm to minimize the contribution of tyrosine fluorescence and the possibility of tyrosine-tryptophan energy transfer. The liposome diameter was kept at 50 nm to minimize light scattering, and the insertion of pHLIPs into the liposomes was triggered by a pH drop from 8 to 3.6. The insertion occurred through three statistically identifiable steps (transitions), and the changes of fluorescence signals were fitted with a four-state model, see details in [17], which assumes a sequential pathway for the processes of insertion that starts from State II and proceeds to final State III via two intermediates:



The characteristic rate constants that were obtained as the result of exponential fittings were related to the real rate constants reflecting three transitions from State I to Int<sub>1</sub>; Int<sub>1</sub> to Int<sub>2</sub>, and Int<sub>2</sub> to State III through a set of equations:

$$k_1 \sim v_1 \quad k_2 \sim \frac{v_2}{1.1} - \frac{v_3}{12.21}, \quad k_3 \sim 0.991v_3$$

where  $v_1, v_2, v_3$  are the characteristic rates of the transitions and  $k_1, k_2, k_3$  are the rate constants (Table 1). The rates for pHLIP insertion to adopt State III decrease with increasing acyl chain length or the presence of 20% of cholesterol in the membrane.

To obtain kinetics activation energies, we monitored changes in tryptophan fluorescence at different temperatures (7°C, 14°C, 18°C, and 25°C) (Figure 4a-c). As expected, increasing the

temperature speeds up the process of insertion for membrane systems of different thickness. To calculate activation energies associated with transitions from one state to another, Arrhenius plots were constructed for each membrane type (Supplementary Figure S5 ) by fitting of the data-points with the linear equation:

$$\ln k = -\frac{E_a}{RT} + \ln A$$

where  $E_a$  is the activation energy and  $A$  is the frequency factor. The total activation energy barriers of pHLIP insertion into 50 nm liposomes composed of  $diC_{14:1}PC$ ,  $diC_{16:1}PC$ , and  $diC_{18:1}PC$  increased with bilayer thickness and were: 36.4 kcal/mol, 40.2 kcal/mol, and 46.8 kcal/mol, respectively (Figure 4d and Table 2). Activation energies of the first step of pHLIP insertion (about 11 kcal/mol) do not depend on the lipid type. The first step is associated with the transition from coil to helical structure on the surface of the lipid bilayer, as was shown previously [17]. The second step is slightly influenced, with a varied activation energy from 13.0 kcal/mol to 12.7 kcal/mol to 14.1 kcal/mol. But, the strongest effects are seen in the final step of pHLIP insertion across the bilayer, which correlate with the lipid bilayer thickness. For  $diC_{14:1}PC$ ,  $diC_{16:1}PC$ , and  $diC_{18:1}PC$  the activation energy barriers are found to be 10.1 kcal/mol, 16.6 kcal/mol, and 21.3 kcal/mol, respectively for the final insertion step across the hydrophobic core of the membrane. It is interesting to note that the frequency factors for the final transition from  $Int_2 \rightarrow$  State III also increased with bilayer thickness ( $\ln A$  in Supplementary Figure S6). The activation barrier for thin bilayers is low, and the probability of the final transition is also low, whereas thicker lipids create a higher activation barrier that is accompanied by a higher rate of transition. These observations might be attributed to the different configurations of the peptide in the initial (adsorbed) State II and the final (inserted) State III in liposomes of different thicknesses. Molecular dynamics calculations might be helpful to reveal atomic positioning of peptides at various states in various lipid systems.

## Discussion

As expected, interactions of a pHLIP with membranes at both high and low pH are perturbed by altering the thickness, curvature and flexibility of lipid bilayers, but now we can reach a greater

understanding of these effects. Deeper partitioning of the peptide is observed with thicker (less flexible/fluid) bilayers (*diC*<sub>20:1</sub>PC and *diC*<sub>22:1</sub>PC) as well as more curved bilayers (50 nm), which is accompanied by formation of helical structures parallel to the membrane surface. While the peptide adopts the transmembrane State III configuration in all bilayer types at low pH, in thick bilayers the lipids can be perturbed by the pHLIP helix caused by a possible “hydrophobic mismatch”: a difference in the thickness of the bilayer core and the length of the peptide's transmembrane domain. Hypothetically, water molecules at the interface of a disturbed bilayer can more readily access the fluorophore's indole ring and quench its fluorescence. The decrease of fluorescence anisotropy in thick bilayers could also be explained by enhanced flexibility of tryptophan residues due to this partial exposure to water molecules where there is a hydrophobic mismatch.

Our previous thermodynamics and kinetics studies indicated that about 200 lipids are perturbed, when unstructured pHLIP occupies membrane surface at pH 8 in State II [15], and about 85% of interfacial helical structure is formed within first ~0.1 sec after pH drop from 8 to 3.6 [18]. We assume that when a peptide forms a rigid helical structure and penetrates deeply into one monolayer of a lipid bilayer, it leads to the disruption of the ordered alignment of lipids, promoting instability and dynamic membrane tension, which presumably drives peptide insertion. The membrane tensions and instability are released when the peptide adopts a transmembrane orientation, when only 10-20 lipids are interacting with helix in State III at low pH [15]. Bilayer curvature and lipid composition would influence that tension, due to the differences in flexibility between thick vs. thin or highly curved vs. planar bilayers. The hydrophobic core of the bilayer represents a barrier for the insertion that requires energy to overcome.

In the kinetics studies of pHLIP insertion into membranes composed of *diC*<sub>14:1</sub>PC, *diC*<sub>16:1</sub>PC and *diC*<sub>18:1</sub>PC lipids, increased lipid acyl chain length is predicted to increase the hydrophobic thickness of the bilayer from 20 Å to 28 Å [29] and decrease membrane fluidity [9] creating higher hydrophobic barrier. The increased content of cholesterol (20%) in liposomes comprised of *diC*<sub>18:1</sub>PC lipids also leads to the increase of bilayer thickness and decrease of membrane fluidity [7]. The rate of pHLIP insertion was correlated with the acyl chain length of the lipid

bilayer and the presence of cholesterol in  $diC_{18:1}PC$  membranes, as the fastest insertion was observed into thinner bilayers ( $diPC_{14:1}$ ) and slowest insertion into thicker bilayers ( $diPC_{18:1}$ ) with 20% cholesterol. The process of pHLIP insertion from State II to State III follows a four-state kinetic model with three transition steps. Step one (interfacial helix formation) do not depend much on the lipid acyl chain length. However, the final step of insertion (translocation of pHLIP's C-terminus across the membrane) increases substantially in activation energy with increasing of lipid bilayer thickness and order. These results correlate with previous studies that showed State II helix formation is independent of the number of protonatable groups at the inserting end of pHLIP, while the time of transmembrane helix formation increases with increasing number of charged groups or presence of cargo in the inserting C-terminus [17]. Thus, the activation barrier for a polypeptide insertion into membrane is affected by i) thickness and fluidity of membrane bilayer and/or ii) by charges and polarity of cargo attached to the peptide inserting end.

It is also important to note, that the process of peptide insertion starts from different pHLIP's "initial configurations" (and potentially slightly different final inserted configurations) for different lipid bilayers. In State II, pHLIPs have more helical structure and deeper penetration into the outer monolayer of bilayers with longer acyl chains and with highly curved membranes [30]. We demonstrated that pHLIP is sensing hydrophobic exposure in the membrane lipids. The exposure results from a combination of two factors: high curvature of the bilayer (SUVs vs LUVs and vs GUVs) and long acyl chains of the lipids that compose this bilayer. Packing defects of the lipid headgroups located on the outer leaflets create the spaces for peptide enhanced binding to membrane.

pHLIPs have been under development for clinical applications due to their tumor targeting activity *in vivo* [19-21, 31, 32]. Their specific accumulation in tumors is thought to primarily result from its differential interaction with membranes at basic vs. acidic pH. The observations we report here allow us to view additional factors that may influence pHLIP targeting in the body or translocation of cargo molecules across bilayers of various membranes within a cell, since peptide insertion could be promoted in membranes with lower thickness and higher fluidity or regions of high curvature. It has been shown that the membrane of human leukemia and



lymphoma cancer cells has increased fluidity, attributed to changes in their phospholipid and cholesterol content [33, 34]. With abnormally high rates of cell division, cancer cells often exhibit such changes in membrane composition as they must upregulate biosynthetic pathways to provide cell building blocks, such as membrane components, rather than relying on circulating supplies. Since biosynthesis-sourced membranes significantly differ from the membrane composition of healthy cells, cancer cells are likely to have an abnormal set of membrane physical properties. While the physical properties of biological membranes are a likely factor influencing the selective targeting of cancer cells by pHLIPs and other membrane-interactive molecules, we find the effects are not dramatically large in our model systems. Nevertheless, local fluidity enhances local curvature in membranes, locally exposing more hydrophobic area in a bilayer. Surface binding of a peptide could be enhanced in tumor cells by such effects.

### **Acknowledgements**

This work was supported by grants from the National Institute of General Medical Sciences of the National Institute of Health under award number GM073857.

### **Declaration of Interest**

OA Andreev, DM Engelman and YK Reshetnyak have founded and have a financial interest in a company, pHLIP, Inc., with the aim of bringing pHLIP technology to the clinic. The company has had no involvement in funding the studies reported here.

## References

1. Wallin, E. and G.V. Heijne, *Genome-wide analysis of integral membrane proteins from eubacterial, archaean, and eukaryotic organisms*. Protein Science, 1998. **7**(4): p. 1029-1038.
2. van Meer, G., D.R. Voelker, and G.W. Feigenson, *Membrane lipids: where they are and how they behave*. Nat Rev Mol Cell Biol, 2008. **9**(2): p. 112-24.
3. McIntosh, T.J. and S.A. Simon, *Roles of bilayer material properties in function and distribution of membrane proteins*. Annu Rev Biophys Biomol Struct, 2006. **35**: p. 177-98.
4. Lee, A.G., *How lipids affect the activities of integral membrane proteins*. Biochim Biophys Acta, 2004. **1666**(1-2): p. 62-87.
5. Lewis, B.A. and D.M. Engelman, *Lipid bilayer thickness varies linearly with acyl chain length in fluid phosphatidylcholine vesicles*. Journal of molecular biology, 1983. **166**(2): p. 211-217.
6. Oldfield, E. and D. Chapman, *Dynamics of lipids in membranes: Heterogeneity and the role of cholesterol*. FEBS letters, 1972. **23**(3): p. 285-297.
7. Subczynski, W.K., et al., *High Cholesterol/Low Cholesterol: Effects in Biological Membranes Review*. Cell Biochem Biophys, 2017.
8. Mitchell, D.C., *Progress in understanding the role of lipids in membrane protein folding*. Biochim Biophys Acta, 2012. **1818**(4): p. 951-6.
9. Anbazhagan, V. and D. Schneider, *The membrane environment modulates self-association of the human GpA TM domain--implications for membrane protein folding and transmembrane signaling*. Biochim Biophys Acta, 2010. **1798**(10): p. 1899-907.
10. Curran, A.R., R.H. Templer, and P.J. Booth, *Modulation of folding and assembly of the membrane protein bacteriorhodopsin by intermolecular forces within the lipid bilayer*. Biochemistry, 1999. **38**(29): p. 9328-36.
11. Seddon, A.M., et al., *Phosphatidylglycerol lipids enhance folding of an alpha helical membrane protein*. J Mol Biol, 2008. **380**(3): p. 548-56.
12. Kleinschmidt, J.H. and L.K. Tamm, *Secondary and tertiary structure formation of the beta-barrel membrane protein OmpA is synchronized and depends on membrane thickness*. J Mol Biol, 2002. **324**(2): p. 319-30.

13. Pocanschi, C.L., et al., *The major outer membrane protein of Fusobacterium nucleatum (FomA) folds and inserts into lipid bilayers via parallel folding pathways*. J Mol Biol, 2006. **355**(3): p. 548-61.
14. Reshetnyak, Y.K., et al., *A monomeric membrane peptide that lives in three worlds: in solution, attached to, and inserted across lipid bilayers*. Biophysical journal, 2007. **93**(7): p. 2363-72.
15. Reshetnyak, Y.K., et al., *Energetics of peptide (pHLIP) binding to and folding across a lipid bilayer membrane*. Proceedings of the National Academy of Sciences, 2008. **105**(40): p. 15340-15345.
16. Musial-Siwiek, M., et al., *Tuning the insertion properties of pHLIP*. Biochimica et Biophysica Acta (BBA)-Biomembranes, 2010. **1798**(6): p. 1041-1046.
17. Karabadzak, A.G., et al., *Modulation of the pHLIP transmembrane helix insertion pathway*. Biophysical journal, 2012. **102**(8): p. 1846-1855.
18. Andreev, O.A., et al., *pH (low) insertion peptide (pHLIP) inserts across a lipid bilayer as a helix and exits by a different path*. Proceedings of the National Academy of Sciences of the United States of America, 2010. **107**(9): p. 4081-6.
19. Andreev, O.A., et al., *Mechanism and uses of a membrane peptide that targets tumors and other acidic tissues in vivo*. Proceedings of the National Academy of Sciences of the United States of America, 2007. **104**(19): p. 7893-8.
20. Viola-Villegas, N.T., et al., *Understanding the pharmacological properties of a metabolic PET tracer in prostate cancer*. Proc Natl Acad Sci U S A, 2014. **111**(20): p. 7254-9.
21. Reshetnyak, Y.K., et al., *Measuring tumor aggressiveness and targeting metastatic lesions with fluorescent pHLIP*. Molecular imaging and biology : MIB : the official publication of the Academy of Molecular Imaging, 2011. **13**(6): p. 1146-56.
22. Karabadzak, A.G., et al., *pHLIP-FIRE, a cell insertion-triggered fluorescent probe for imaging tumors demonstrates targeted cargo delivery in vivo*. ACS Chem Biol, 2014. **9**(11): p. 2545-53.
23. Sosunov, E.A., et al., *pH (low) insertion peptide (pHLIP) targets ischemic myocardium*. Proc Natl Acad Sci U S A, 2013. **110**(1): p. 82-6.

24. Reshetnyak, Y.K., Y. Koshevnik, and E.A. Burstein, *Decomposition of protein tryptophan fluorescence spectra into log-normal components. III. Correlation between fluorescence and microenvironment parameters of individual tryptophan residues.* Biophysical journal, 2001. **81**(3): p. 1735-1758.
25. Wallimann, P., et al., *Dual wavelength parametric test of two-state models for circular dichroism spectra of helical polypeptides: anomalous dichroic properties of alanine-rich peptides.* J Am Chem Soc, 2003. **125**(5): p. 1203-20.
26. Kwok, S.C. and R.S. Hodges, *Stabilizing and destabilizing clusters in the hydrophobic core of long two-stranded alpha-helical coiled-coils.* J Biol Chem, 2004. **279**(20): p. 21576-88.
27. Burck, J., et al., *Oriented Circular Dichroism: A Method to Characterize Membrane-Active Peptides in Oriented Lipid Bilayers.* Acc Chem Res, 2016. **49**(2): p. 184-92.
28. Wu, Y., H.W. Huang, and G.A. Olah, *Method of oriented circular dichroism.* Biophys J, 1990. **57**(4): p. 797-806.
29. Lewis, B.A. and D.M. Engelman, *Lipid bilayer thickness varies linearly with acyl chain length in fluid phosphatidylcholine vesicles.* J Mol Biol, 1983. **166**(2): p. 211-7.
30. Barrera, F.N., J. Fendos, and D.M. Engelman, *Membrane physical properties influence transmembrane helix formation.* Proc Natl Acad Sci U S A, 2012. **109**(36): p. 14422-7.
31. Cruz-Monserrate, Z., et al., *Targeting pancreatic ductal adenocarcinoma acidic microenvironment.* Sci Rep, 2014. **4**: p. 4410.
32. Macholl, S., et al., *In vivo pH imaging with (99m)Tc-pHLIP.* Mol Imaging Biol, 2012. **14**(6): p. 725-34.
33. Sherbet, G.V., *Membrane fluidity and cancer metastasis.* Exp Cell Biol, 1989. **57**(4): p. 198-205.
34. Kiss, C., M. Balazs, and I. Keri-Fulop, *Dexamethasone decreases membrane fluidity of leukemia cells.* Leuk Res, 1990. **14**(3): p. 221-5.

## Tables

**Table 1.** The rate constants ( $k$ ,  $\text{sec}^{-1}$ ) characterizing transitions from State I to Int<sub>1</sub>; Int<sub>1</sub> to Int<sub>2</sub>, and Int<sub>2</sub> to State III along pHLIP insertion pathway into the lipid bilayer of liposomes of various lipid compositions and cholesterol content.

	<b>14:1 PC</b>	<b>16:1 PC</b>	<b>18:1 PC</b>	<b>18:1 PC 20% chol.</b>
$k_1$	57	77	103	100
$k_2$	3.4	3.1	4.9	1.9
$k_3$	0.14	0.13	0.06	0.01

**Table 2.** The values of the activation energies ( $E_a$ , kcal/mol) and St. Er. were calculated for the transitions from State I to Int<sub>1</sub>; Int<sub>1</sub> to Int<sub>2</sub>, and Int<sub>2</sub> to State III along pHLIP insertion pathway into the lipid bilayer of liposomes of various lipid compositions by fitting of rates (Supplementary Figures S5) with Arrhenius function.

<b>Transitions</b>	<b>14:1 PC</b>	<b>16:1 PC</b>	<b>18:1 PC</b>
<b>State II → Int<sub>1</sub></b>	11.4 ± 1.7	10.9 ± 1.3	11.4 ± 1.5
<b>Int<sub>1</sub> → Int<sub>2</sub></b>	13.0 ± 1.0	12.7 ± 2.4	14.1 ± 2.3
<b>Int<sub>2</sub> → State III</b>	10.1 ± 2.2	16.6 ± 0.9	21.3 ± 2.2
<b>Total: State II → State III</b>	<b>34.6</b>	<b>40.2</b>	<b>46.8</b>

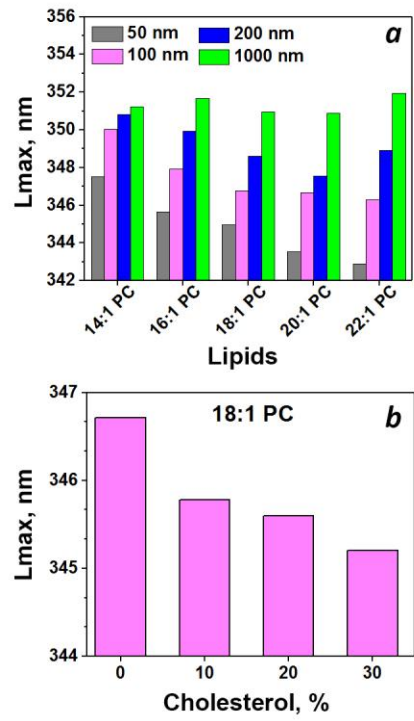
## Figure Legends

**Figure 1. pHLIP interaction with membranes of different curvature and cholesterol content at pH 8.** The position of maximum ( $L_{max}$ ) of fluorescence spectra of pHLIP measured at pH 8.0 in the presence of liposomes of various lipid compositions,  $diC_{14:1}PC$ ,  $diC_{16:1}PC$ ,  $diC_{18:1}PC$ ,  $diC_{20:1}PC$   $diC_{22:1}PC$  and various sizes from 50 to 1000 nm in diameter (**a**), and  $diC_{18:1}PC$  liposomes of 100 nm in diameter with varying amount of cholesterol (**b**).

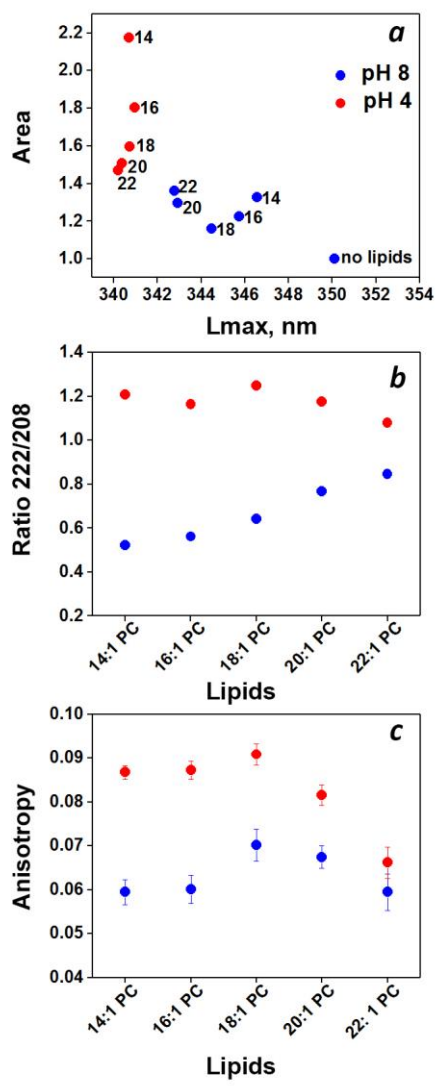
**Figure 2. pHLIP interaction with membranes of different thickness at pH 8 and pH 4.** (**a**) The relation between normalized area under the pHLIP fluorescence spectra and position of maxima of emission ( $L_{max}$ ) are shown. The fluorescence intensity was normalized for the intensity of 2  $\mu M$  of pHLIP in solution without liposomes. Numbers next to the points denote the acyl chain length of the lipids. Fluorescence spectra of pHLIP in different states are shown in Supplementary Figure S2a. (**b**) Ratio of ellipticity at 222 nm and 208 nm of pHLIP measured in the presence of liposomes of various lipid compositions are presented. CD spectra of pHLIP in different states are shown in Supplementary Figure S2b. (**c**) Anisotropy of pHLIP tryptophan fluorescence measured at 350 nm in the presence of liposomes of various lipid compositions are shown, error bars, s.d. ( $n = 10$  experiments). Peptide and lipid concentrations were 2  $\mu M$  and 0.4 mM consequently, and an average liposome diameter was 50 nm in all measurements. The data obtained at pH 8 and pH 4 are shown in blue and red, respectively.

**Figure 3. Oriented circular dichroism of pHLIP.** OCD spectra of pHLIP interacting with  $diC_{14:1}PC$  (**a**),  $diC_{18:1}PC$  (**b**) and  $diC_{22:1}PC$  (**c**) lipid membranes at pH 3.6 are shown.

**Figure 4. Insertion kinetics of pHLIP across different bilayers at different temperatures and calculated activation energies.** Kinetics of pHLIP insertion across the lipid bilayer of 50 nm liposomes comprising of  $diC_{14:1}PC$  (**a**),  $diC_{16:1}PC$  (**b**), and  $diC_{18:1}PC$  (**c**) lipids were monitored by changes of tryptophan fluorescence of pHLIP as a result of pH jump from 8.0 to 3.6 at different temperatures. Activation energy,  $E_a$ , and St. Er. were calculated for the transitions between four states along pHLIP insertion pathway by fitting of rates (Supplementary Figures S5) with Arrhenius function (**d**). The activation energy values are given in Table 2.

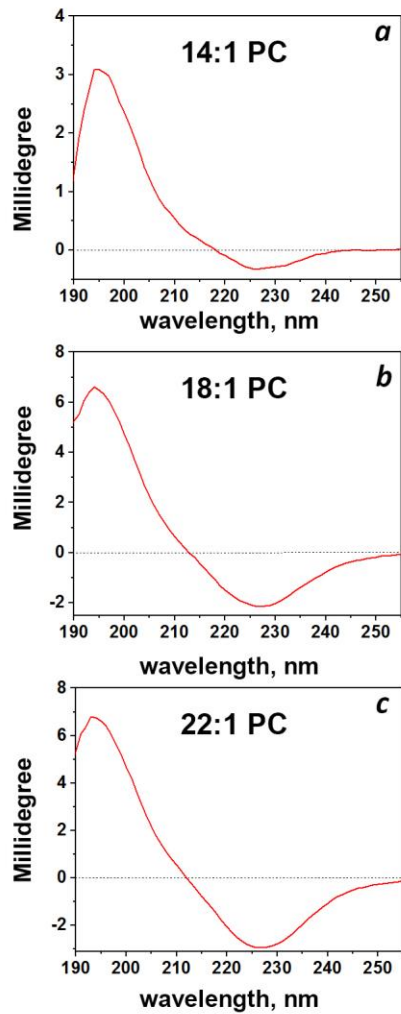


**Figure 1**

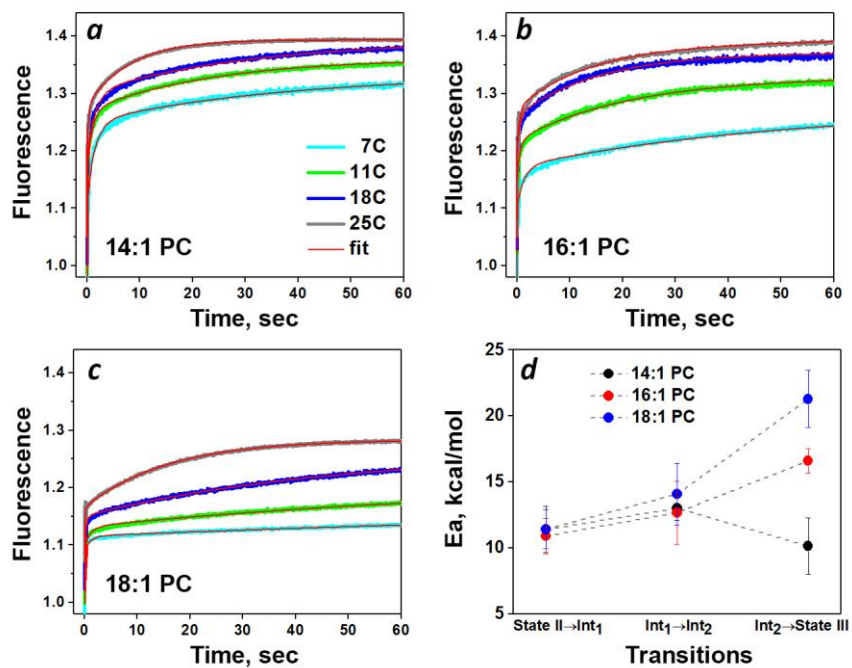


**Figure 2**





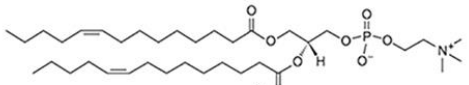
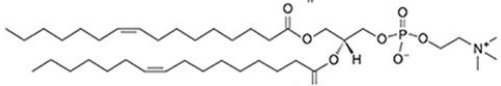
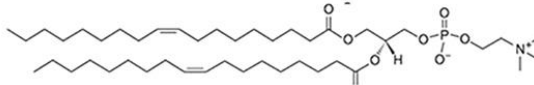
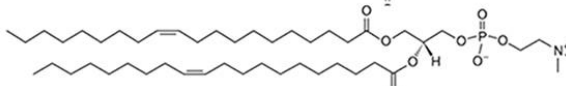
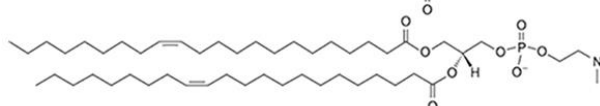
**Figure 3**



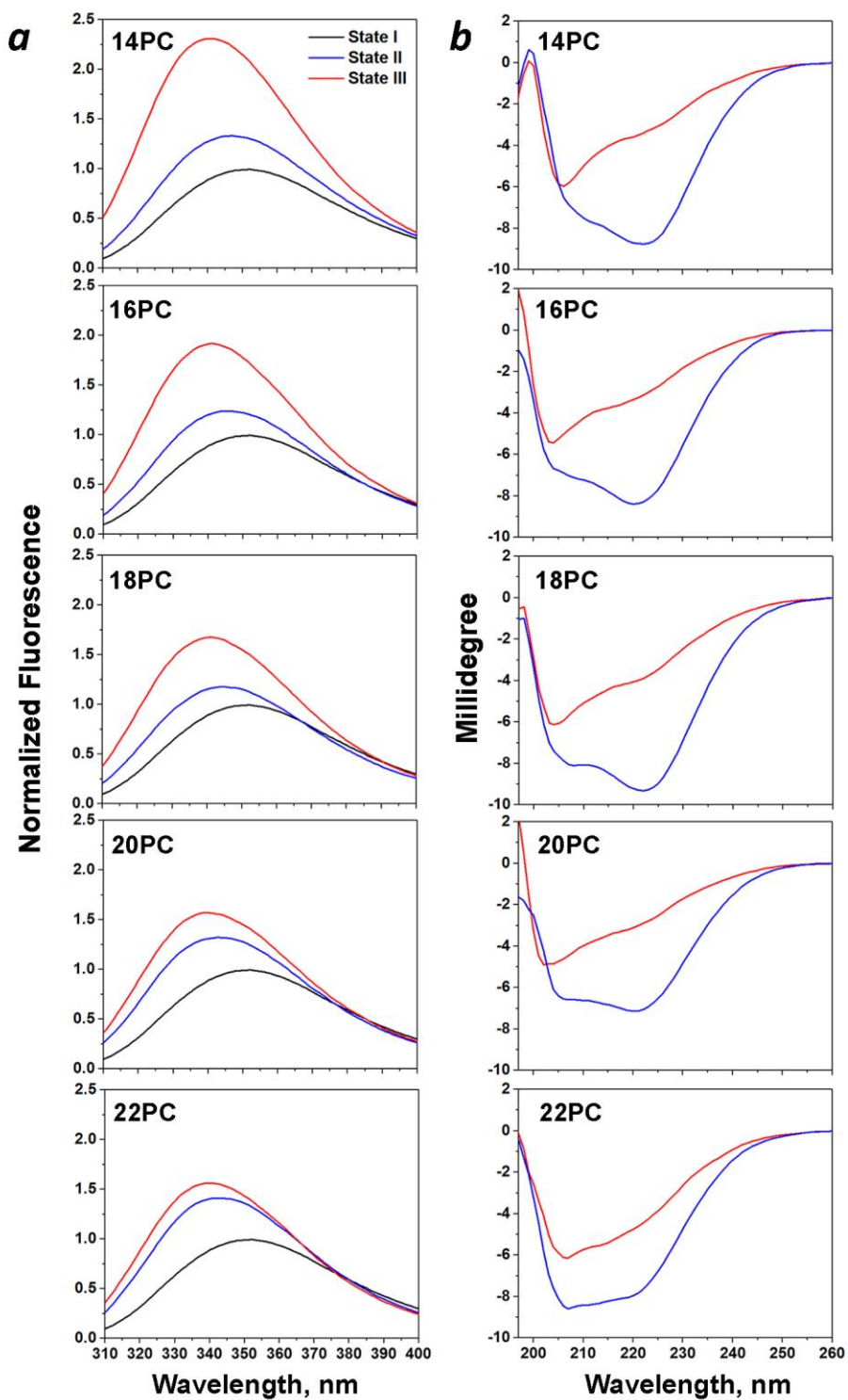
**Figure 4**

## Supplementary Information

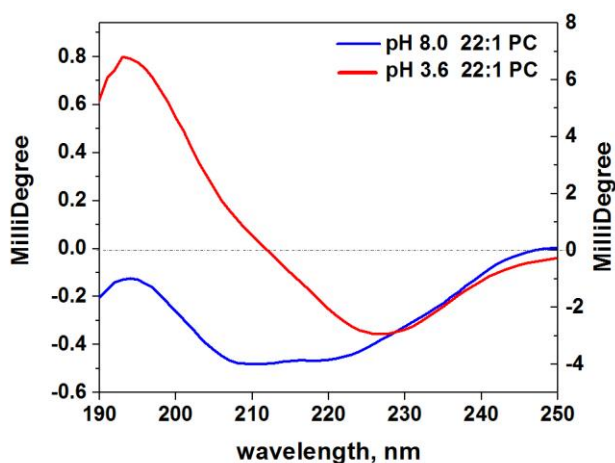
### Bilayer thickness and curvature influence binding and insertion of pHLIP<sup>®</sup> peptide

	Lipids	T <sub>m</sub> (C)
	14:1 (Δ9-Cis)PC	-
	16:1 (Δ9-Cis)PC	-36
	18:1 (Δ9-Cis)PC	-20
	20:1 (Δ11-Cis)PC	-4
	22:1 (Δ13-Cis)PC	11

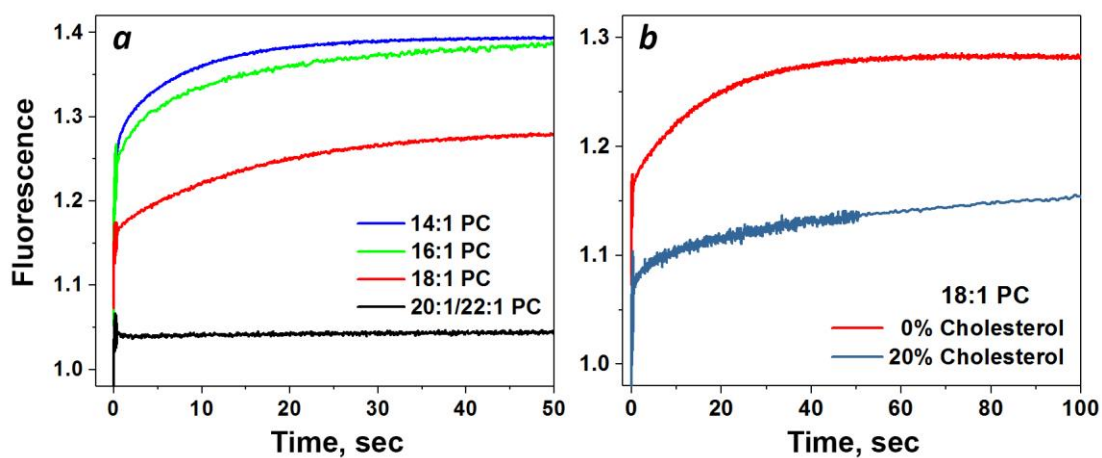
**Supplementary Figure S1.** Chemical structures and melting temperatures of monounsaturated lipids used in the study.



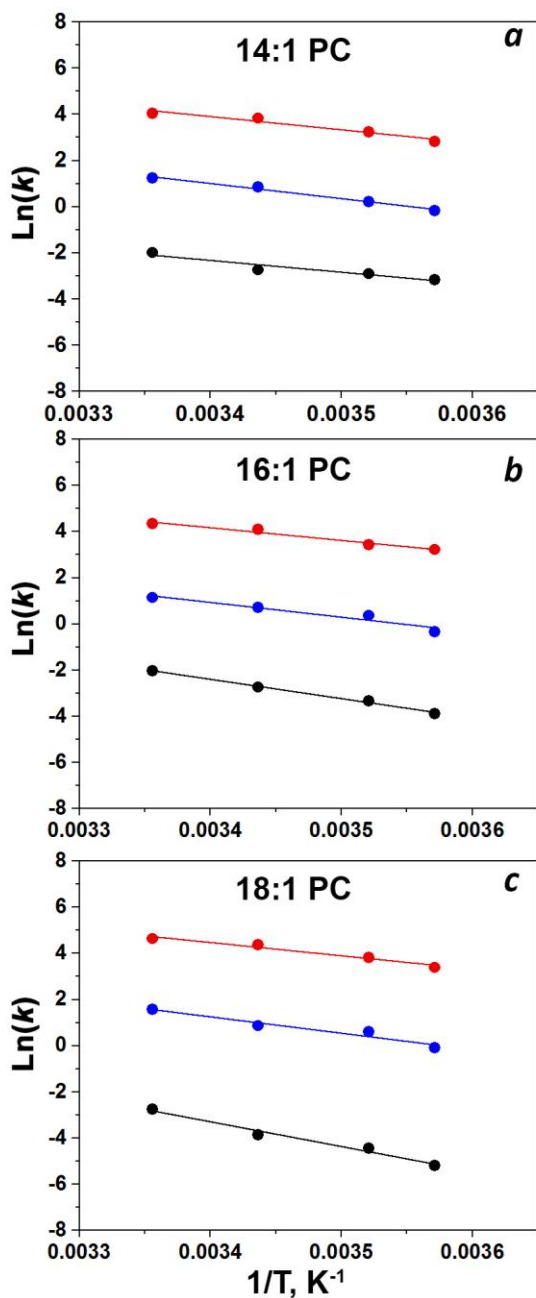
**Supplementary Figure S2.** Tryptophan fluorescence (*a*) and circular dichroism (*b*) spectra of pHLIP measured in State I at pH 8.0 in absence of POPC liposomes (black lines), State II at pH 8.0 in presence of POPC liposomes (blue lines) and State III at pH 3.6 in presence of POPC liposomes (red lines).



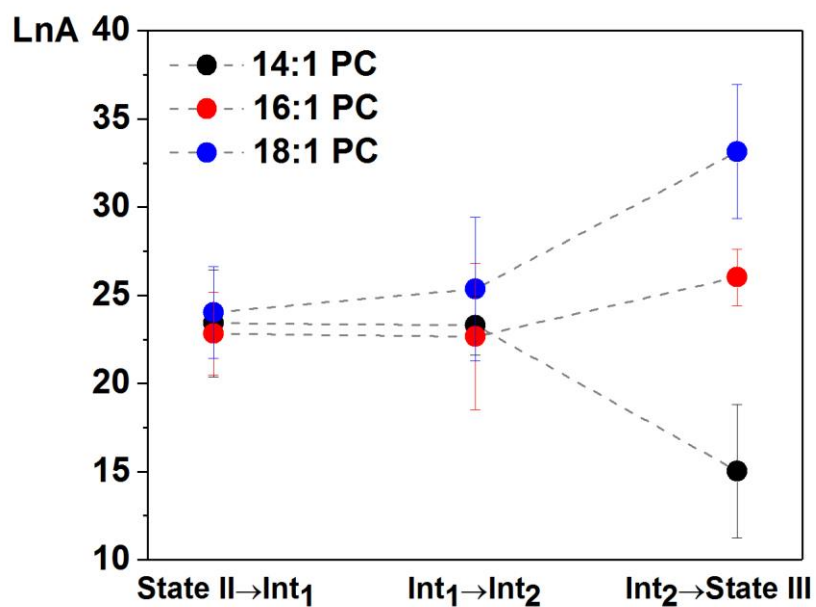
**Supplementary Figure S3.** Oriented circular dichroism of pHLIP in 22:1 PC membranes at different pHs. Left Y-axis shows values for pH 8.0 signal, right Y-axis shows values for pH 3.6 signal.



**Supplementary Figure S4.** Kinetics of pHLIP insertion across the lipid bilayer of 50 nm liposomes of various lipid compositions (*a*) and cholesterol content (*b*) were monitored by changes of tryptophan fluorescence of pHLIP as a result of pH jump from 8.0 to 3.6. The kinetic parameters are presented in Table 1.



**Supplement Figure S5.** The Arrhenius plots for pHLIP insertion across the  $diC_{14:1}PC$  (a),  $diC_{16:1}PC$  (b), and  $diC_{18:1}PC$  (c) lipid bilayers are shown. Rates were obtained by fitting of the experimental kinetics data shown on Figure 4a-c employing four-state kinetic models, which assumes a sequential pathway for the processes of peptide insertion with 3 transitions State I  $\rightarrow$  Int<sub>1</sub>; Int<sub>1</sub>  $\rightarrow$  Int<sub>2</sub> and Int<sub>2</sub>  $\rightarrow$  State III described by 3 rates,  $k_i$  ( $k_1$  is shown in red,  $k_2$  - in blue and  $k_3$  - in black). The Arrhenius plots were obtained by linear fitting and activation energy values were calculated (values are given in Table 2).



**Supplement Figure S6.** The changes of Arrhenius frequency factor,  $A$ , and St. Er. were calculated for the transitions between four states along pHLIP insertion pathway by fitting of rates (Supplementary Figures S5) with Arrhenius function.